
The 3-dimensional effects of distracting magnetically controlled growing rods

1

Authors: ¹Jason Pui Yin Cheung, MBBS, MMedSc, MS, PDipMDPath, FRCS, FHKAM, FHKCOS

¹Prudence Wing Hang Cheung, BSc(Hons)

¹Kenneth MC Cheung, MBBS, MD, FRCS, FHKAM, FHKCOS

Affiliations: ¹Department of Orthopaedics and Traumatology, The University of Hong Kong, Pokfulam, Hong Kong SAR, China

Disclosure: The authors have no financial or competing interests to disclose.

Ethics: Permission to reproduce copyrighted materials or signed patient consent forms granted. The study was approved by the local institutional review board (UW 16-336)

Funding: This study was supported by the Scoliosis Research Society.

Correspondence: Jason Pui Yin Cheung

Department of Orthopaedics & Traumatology

The University of Hong Kong

Professorial Block, 5th Floor

102 Pokfulam Road, Pokfulam

Hong Kong, SAR, China

Tel: (+852) 2255-4581

Fax: (+852) 2817-4392

Email: cheungjp@hku.hk

1

Author	Author roles
Jason Pui Yin Cheung	Study conception and design, data acquisition, analysis, interpretation of data, drafting manuscript, and final approval of published version
Prudence Wing Hang Cheung	Study acquisition and analysis, interpretation of data, revising manuscript, and final approval of published version
Kenneth MC Cheung	Interpretation of data, revising manuscript and final approval of the version to be published

2

The effect of Magnetically Controlled Growing Rods on 3-dimensional changes in deformity correction

Abstract

Study Design: Prospective radiographic study.

Objectives: To determine the 3-dimensional (3D) changes in deformity correction with magnetically controlled growing rod (MCGR) distractions.

Summary of background data: MCGRs can achieve similar coronal plane correction as traditional growing rods. The changes in the sagittal and axial planes are unknown and should be studied as these factors reflect potential for proximal junctional kyphosis and rotational deformity. Frequent MCGR distractions may potentially improve axial plane deformities to the same extent as coronal and sagittal plane deformities.

Methods: Early onset scoliosis (EOS) patients who underwent dual MCGRs with minimum 2-year follow-up were included in this study. 3D reconstructions of 6-monthly biplanar images were used to study changes in coronal, sagittal and axial planes. Changes in growth parameters (body height and arm span) were scaled to changes in coronal Cobb angles, sagittal profile (T1-12, T4-12, L1-L5, L1-S1), and rotational profile at the proximal thoracic, main thoracic and lumbar curves, and pelvic parameters (sagittal pelvic tilt, lateral pelvic tilt and pelvis rotation).

Results: A total of 10 EOS patients were studied. The mean age at index surgery was 8.2 ± 3.0 years and mean postoperative follow-up of 34.3 ± 9.5 months. Six patients had rod exchange at mean 29.5 ± 11.8 months after initial implantation. Despite consistent gains in body height and arm

span, the main changes in coronal and rotational profiles only occurred at the initial rod implantation surgery with only small changes occurring with subsequent follow-ups. Patients with proximal junctional kyphosis had higher preoperative proximal junctional angles and flattening of the sagittal plane occurred at initial surgery with early rebound. No changes in pelvic parameters were observed.

Conclusions: The 3D changes with MCGR are mainly observed with initial rod implantation and no significant changes are observed with distractions. The MCGR can prevent deformity progression in the axial plane.

Level of Evidence: IV

Key Points

1. The rotational correction is greatest with the initial magnetically controlled growing rod implantation and is stable thereafter with distractions.
2. Patients with proximal junctional kyphosis had higher preoperative proximal junctional angles with flattening of the sagittal alignment with rod implantation followed by early rebound.
3. Patients without proximal junctional kyphosis had smaller preoperative proximal junctional angles that were preserved with rod implantation and stable thereafter with distractions.
4. No significant changes in coronal, sagittal or axial plane deformities occur with distractions up to 4 years follow-up.

1 **The effect of Magnetically Controlled Growing Rods on 3-dimensional changes in deformity**
2 **correction**

3

4 **Introduction**

5 Early onset scoliosis (EOS) requires early treatment as they occur in young children with
6 significant remaining growth potential. Left untreated, these deformities are at risk of rapid
7 progression, cosmetic disfigurement and pulmonary insufficiency.[1-3] Growing rods is one of the
8 most common treatment methods for EOS that allow for physiological spine growth while
9 preventing spine deformity progression.[4-6] Traditionally, these rods require open distraction
10 surgeries every 6 months. However, repeated surgeries in a growing child has significant
11 drawbacks including increased risk for anesthetic and wound complications.[1,7] In response to
12 these limitations, a remotely distractible, magnetically controlled growing rod (MCGR) has been
13 developed to allow for outpatient gradual lengthening.[8] The MCGR allows for safe distractions
14 and continuous neurological monitoring in an awake patient. Clinical and radiological outcomes
15 have been shown to be similar to traditional growing rods[8-15] and it has also been used in safe
16 gradual correction of severe spinal deformities.[16,17] The MCGR also allows for non-invasive
17 radiation-free monitoring[18,19] and is an overall less costly option for EOS.[20-22]

18 In terms of curve correction, most studies have showed that the largest amount of coronal curve
19 correction occurs at implantation with subsequent satisfactory control of the deformity.[8,9,12]
20 Despite these coronal changes, assessment of vertebral rotation is important for prognosis as
21 scoliosis is a 3-dimensional (3D) deformity.[23-25] The apical vertebral rotation (AVR) is
22 particularly important with relevance to the rib hump which is a cosmetic concern. An increased
23 rotational deformity may also lead to reduced chest cage area and thus pulmonary compromise.

1 However, the changes in the axial plane with MCGR treatment is unknown due to limitations in
2 imaging availability. Computed tomography (CT) measurements are most useful for measuring
3 vertebral rotation as they provide the true rotational profile of the spine.[26,27] However, it is not
4 routinely performed in children due to high radiation exposure and lack of weight-bearing
5 information.

6 Using the low-dose x-ray device EOS® (EOS® Imaging, Paris, France), we can obtain 3D
7 reconstructed images of the spine based on biplanar images in posteroanterior (PA) and lateral
8 standing views. The EOS® has already been shown to have good reliability for intraobserver and
9 interobserver measurements for scoliosis curves with good precision (2-4 degrees variation only
10 for vertebral rotation).[28-30] Verification of the reconstructed 3D images with CT has already
11 been performed and is shown to be reliable.[31] Thus, it is timely at this stage to assess the effect
12 of gradual distractions with the MCGR on correction of vertebral rotation. 3D models of the spine
13 are created to monitor the change in vertebral rotation with each distraction. This technique can
14 also observe for any relationship between frequent distractions, spine length gain and transverse
15 vertebral growth. Hence, the objective of this study is to determine the 3D corrections of EOS with
16 MCGR distractions.

17

18 **Materials and Methods**

19 *Study design*

20 This was a prospective radiographic study of patients with EOS who underwent dual
21 MCGRs. Patients were recruited consecutively from a tertiary spine referral center since October
22 2015. None of the patients had prior treatment for their spinal deformity. All patients had major
23 thoracic deformities, at least 2 years follow-up after their primary insertion of MCGRs, and images

1 coupled with recorded body habitus parameters (body height, arm span, body weight). For all
2 patients, dual MCGRs of 5.5 millimetres in diameter were placed in a standard and offset
3 configuration. Ethics was approved by the local institutional review board. All patients underwent
4 monthly 2mm distractions to both rods starting at 2 months after MCGR implantation.

5

6 *3D reconstruction*

7 Radiographic images were obtained of recruited subjects using EOS® imaging every 6-
8 months of follow-up to assess for longitudinal changes in parameters. The EOS® system is a slot-
9 scanning radiographic device that utilizes two x-ray sources to allow simultaneous capture of both
10 the PA and lateral images. It reduces the radiation to up to 9 times compared to conventional
11 radiographs.[32] Two pairs of detectors are positioned so that the images can be generated line by
12 line as the scanning proceeds vertically. Patients stand in the machine so images are taken in
13 weight-bearing position. Scan time lasts for 8 to 15 seconds according to the patient's height. The
14 reconstruction of the spine is based on available models provided by the EOS® company.[29] The
15 image reconstruction procedure is as follows: Firstly, the pelvic anatomical landmarks are accessed.
16 The two spheres of the acetabuli are identified as well as the sacral endplate. Then, the spinal curve
17 from the T1 upper endplate to the L5 lower endplate is identified. The approximate borders of the
18 spine vertebra are identified and a preliminary model is created. Fine adjustment of the model is
19 performed by manipulating the points on the four corners of the vertebral body, pedicles and
20 posterior arches from T1 to L5.[33] Each modification improves the accuracy of the model. Finally,
21 the accepted changes will create the 3D model with the necessary angles provided automatically
22 (**Figure 1**). The two-dimensional images of the whole body had undergone 3-D reconstructions of
23 the spine and lower limb using the validated SterEOS® software (EOS® Imaging, Paris, France).

1 Trained individuals blinded to the clinical information performed all image reconstructions. The
2 time spent on 3D modelling was 31.7 ± 6.1 minutes per reconstruction.

3

4 *Study parameters*

5 Demographic data including patient gender, age at MCGR implantation, and diagnosis
6 (congenital, neuromuscular, syndromic, idiopathic) was recorded. Changes in body height (cm),
7 body weight (kg), arm span (cm), and body mass index were recorded. Images were obtained
8 preoperatively, immediate postoperatively, and from postoperative 6-months to postoperative-48
9 months at 6-monthly intervals. Details regarding the primary surgery included levels of
10 instrumentation and anchor-type (pedicle screw or hook). Any complications such as infection,
11 anchor loosening, and proximal junctional kyphosis (PJK) were recorded. The number of rod
12 exchanges was also recorded.

13 Specifically for the 3D imaging parameters, in addition to the gross morphology of the 3D
14 model, the SterEOS® software provided the usually quoted spinopelvic alignment parameters.[34]
15 These included the coronal Cobb angle, T1-T12 kyphosis, T4-T12 kyphosis, L1-S1 lordosis, L1-
16 L5 lordosis, pelvic incidence, sagittal and lateral pelvic tilt, pelvic rotation and sacral slope. The
17 rotational profile was also studied through the measurement of apical vertebral rotation at the
18 thoracic apex, the proximal thoracic apex and the lumbar apex. PJK was identified by an increase
19 in the proximal junctional angle (caudal endplate of the UIV to the cephalad endplate of two
20 vertebrae proximally) of 10 degrees or more and at least 10 degrees greater than the preoperative
21 measurement.[35]

22

23 *Statistical Analysis*

1 Descriptive statistics were calculated in mean, standard deviation (SD) and percentage.
2 Mean values were plotted against follow-up time-points, enabling comparison between
3 parameters. The timing of rod exchanges was also taken into account and was expressed using bar
4 graphs within the dual-axis plot. Normality tests using Shapiro-Wilk tests were run and found that
5 data was not normally distributed. One-way analysis of variance (ANOVA) was used to study the
6 changes in radiographical parameters with time. Spearman correlation test was used to assess for
7 any correlation between changes of the axial, coronal and sagittal parameters. Spearman's rank
8 correlation coefficient (r_s) depicts the direction and strength of any relationships detected, with a
9 value of 0.10 to 0.29 suggesting a small association, whereas a coefficient of 0.30 to 0.49 and \geq
10 0.50 indicating a medium and a large association respectively.[36] Statistical analyses were
11 conducted using SPSS Windows 23.0 (IBM SPSS Inc., Chicago, Illinois, USA) and charts were
12 created by Excel (Microsoft, Redmond, Washington, USA). A p-value of <0.05 was considered
13 statistically significant.

14

15 **Results**

16 A total of 10 (2 males, 8 females) EOS patients (**Table 1**) were studied. Their diagnoses
17 were juvenile idiopathic (n=5), infantile idiopathic (n=1), neurofibromatosis (n=1), neuromuscular
18 (n=1), Sotos syndrome (n=1) and Arthrogyriposis (n=1). The mean age at index surgery was
19 8.2 ± 3.0 years and mean postoperative follow-up of 34.3 ± 9.5 months. Six patients had rod
20 exchanges. The baseline profile of the patients is listed in **table 2**. The preoperative body height
21 was 122.7 ± 10.2 cm, preoperative arm span was 118.8 ± 12.8 cm, preoperative body weight was
22 20.8 ± 7.1 kg, and preoperative body mass index was 13.0 ± 2.9 kg/m². The pelvic incidence and

1 lumbar lordosis was well-matched preoperatively. No significant proximal thoracic deformity was
2 observed in coronal, sagittal or axial planes.

3 Consistent gains in body height, body weight, and arm span were observed with follow-up
4 (**Table 3**). The main changes in coronal Cobb angles only occurred at the initial rod implantation
5 surgery with only small changes that occurred at subsequent follow-ups. For the sagittal plane, the
6 spine was flattened with initial surgery with reductions in T1-T12 and T4-T12 kyphosis, and L1-
7 S1 and L1-L5 lordosis. There was rebound increases in kyphosis and lordosis within the two years
8 of follow-up followed by minimal changes thereafter. The lateral pelvic tilt maintained its position
9 throughout follow-up while sagittal pelvic tilt gradually reduced to more retroversion especially
10 in the first two years of follow-up. When comparing preoperative, immediate postoperative and
11 final follow-up data (**Table 4**), the main changes only occurred for thoracic and lumbar Cobb
12 angles, L1-S1 lordosis.

13 For the axial plane, the apical vertebral rotation also had its largest change in the initial rod
14 implantation without significant changes following subsequent distractions (**Figure 2**) despite
15 increasing body height. There was minimal change overall in the rotational profiles, even after rod
16 exchanges. For the thoracic apex, which had the largest changes, besides the initial surgery, the
17 maximum mean change was only 3.4 ± 3.5 degrees thereafter. Similarly, the lumbar apex and
18 proximal thoracic apex had maximal mean changes of 4.3 ± 6.8 degrees and 3.4 ± 3.5 degrees,
19 respectively. Further analyses performed comparing the three parameters showed no significant
20 correlations between coronal, sagittal and axial plane changes except for changes in coronal
21 parameters and T1-12 kyphosis and L1-L5 lordosis (**Table 5**).

22 There were three patients who developed PJK (**Table 5**). These patients had preoperatively
23 larger proximal junctional angles than those without PJK, and their kyphotic angles were flattened

1 with initial rod implantation (**Table 6**). PJK occurred as early as postoperative 6 months (**Figure**
2 **3**) but was sustained throughout follow-up without deterioration.

3

4 **Discussion**

5 Understanding changes in 3D is crucial for proper management of patients with EOS.
6 Rotational malalignment may aggravate the rib hump, which is a major concern for cosmesis.
7 Increasing rotational deformities may also reduce the area of the chest cage thereby compromising
8 pulmonary function. In this study, we explored the potential 3D changes that occur with MCGR
9 treatment for EOS. Like the coronal Cobb angle, the main changes occur in the initial rod
10 implantation without significant variations with distractions. Hence, the rotational profile is also
11 be maintained with MCGR treatment.

12 Axial plane rotation is commonly measured on plain radiographs by Perdriolle and Vidal's
13 method.[37,38] However, 3D assessment based on a single 2-dimensional image is inherently
14 inaccurate as each scoliosis is unique with complexities that are not easily identified.[39] 3D
15 reconstruction using the EOS® is accurate to within 4-6 degrees for the coronal deformity and 2-
16 4 degrees for vertebral rotation in scoliosis.[28,29] Verification of these reconstructed 3D images
17 has been performed with CT and is proven to be reliable.[31] It is important to note that the time
18 required to complete each 3D reconstruction was 31.7 ± 6.1 minutes. Despite the advantages of
19 reduced radiation exposure, major drawbacks of using EOS® reconstructions is the manpower
20 requirement and lack of automation which we hope will be solved in the future. Nevertheless, this
21 is the best 3D assessment tool available currently.

22 The changes in the axial plane concerning growing rods are not well understood. Kamaci *et*
23 *al*[38] suggested that the apical vertebral rotation improves with traditional growing rod treatment

1 by comparing the preoperative and final follow-up assessments. However, this does not reflect the
2 changes occurring with distractions and the interplay with events like rod complications or rod
3 exchanges. The 10 degree improvements reported in their study is similar to our findings of mean
4 13.6 degree reduction in rotation after MCGR implantation.[38] With the previous reports of
5 similar initial corrections in the coronal plane after traditional growing rod and MCGR
6 implantation[4,9,12-15], we speculate that the reported improvements elsewhere was contributed
7 by the initial surgery rather than with distraction. Nevertheless, it is important to note that no
8 deterioration in the rotational profile was observed during the course of the treatment. Hence,
9 MCGR is successful in preventing axial plane deformity progression despite no anchors around
10 the apex of the deformity.

11 The comparable changes found with rod implantation and with distractions in 3D is
12 representative of spinal coupling.[40-42] During MCGR implantation, no particular maneuver was
13 performed to correct the apical rotation as there are only two sets of anchors placed at the proximal
14 and distal foundations without any instrumentation in the intervening spinal segments or attempt
15 to derotate the spine. Hence, effectively only the coronal deformity is planned for correction with
16 rod insertion and intraoperative distraction maneuvers. The spontaneous reduction of the rotational
17 deformity is achieved through coupling.

18 An interesting phenomenon is observed for the sagittal plane. Proper contouring of the MCGR
19 is not easily achievable due to the straight actuator segment.[12,30] This has been attributed to the
20 high-risk of PJK after growing rod surgery.[30,43,44] The ability of the spine to compensate for
21 sudden flattening of the sagittal alignment is highlighted by the early rebound in thoracic kyphosis
22 and lumbar lordosis after rod implantation. PJK may occur and in our series, it is apparent for those
23 with preoperative higher proximal junctional angles. The recruitment of more cranial spinal

1 segments to reproduce the thoracic kyphosis is clearly represented by a rebound increase in
2 proximal junctional angle as early as postoperative 6 months. There is also greater T1-T12
3 kyphotic change as compared to T4-T12. The inclusion of T1-4 in addition to the T4-T12 better
4 incorporates the kyphotic changes occurring in the proximal thoracic spinal segments. In our
5 series, the increase in kyphosis was only observed in the early postoperative follow-up and the
6 overall kyphosis did not change thereafter. There is no further deterioration in the proximal
7 junctional angle after the early change. This may be a reason why we only observed three patients
8 developing PJK, which is a relatively low rate (30%) as compared to previous reports
9 (~40%).[15,43]

10 There are several limitations to this study that must be discussed. Firstly, we report the results
11 of a small number of patients with variable ages at rod implantation. The lack of significance
12 reported by the correlation analyses may be related to these limitations. However, it may also
13 represent the variations in 3D curve types that have been reported.[39] For example, not all
14 scoliosis curves are hypokyphotic and as correlation analyses are uni-directional, this tool may not
15 be most representative of interactions between coronal, sagittal and axial planes. Nevertheless, our
16 results will need to be validated in a larger study. For the purposes of this study, despite the
17 presence of implants superimposing onto the vertebral bodies, measurements using the EOS® is
18 still possible for postoperative images with reproducible data.[34] However, in one study
19 investigating 3D reconstructions of the spine with posterior instrumentation in-situ, the reported
20 precision may vary from 2.8 to 10 degrees for Cobb angles and 6.8 to 10.4 degrees for apical
21 vertebral rotation calculations. At present, we unfortunately have no other more accurate 3D
22 assessment available for children that also avoids the high radiation exposure associated with CT.

1 This is the first study to assess 3D changes in scoliosis correction with MCGR distractions.
2 The corrections in rotational deformity are seen only with initial rod implantation and no
3 significant changes are observed with distractions thereafter. Hence, the MCGR is successful in
4 controlling the deformity and prevents its progression in the coronal, sagittal and axial planes.
5 Understanding 3D changes in the deformity is important as it provides insight into how growth-
6 sparing distraction devices can be tailored towards different patients with variable curve types.
7 Further study can examine whether transverse plane growth deviates with MCGR treatment and
8 whether this influences the correction outcomes achieved at final fusion surgery, as well as
9 correlation with respiratory function.

1 **References**

- 2 1. Akbarnia BA, Emans JB. Complications of growth-sparing surgery in early onset scoliosis.
3 *Spine (Phila Pa 1976)* 2010;35:2193-204.
- 4 2. Bess S, Akbarnia BA, Thompson GH, et al. Complications of growing-rod treatment for
5 early-onset scoliosis: analysis of one hundred and forty patients. *The Journal of bone and joint*
6 *surgery American volume* 2010;92:2533-43.
- 7 3. Redding GJ, Mayer OH. Structure-respiration function relationships before and after
8 surgical treatment of early-onset scoliosis. *Clin Orthop Relat Res* 2011;469:1330-4.
- 9 4. Akbarnia BA, Breakwell LM, Marks DS, et al. Dual growing rod technique followed for
10 three to eleven years until final fusion: the effect of frequency of lengthening. *Spine (Phila Pa*
11 *1976)* 2008;33:984-90.
- 12 5. Akbarnia BA, Marks DS, Boachie-Adjei O, Thompson AG, Asher MA. Dual growing rod
13 technique for the treatment of progressive early-onset scoliosis: a multicenter study. *Spine (Phila*
14 *Pa 1976)* 2005;30:S46-57.
- 15 6. Winter RB, Moe JH, Lonstein JE. Posterior spinal arthrodesis for congenital scoliosis. An
16 analysis of the cases of two hundred and ninety patients, five to nineteen years old. *J Bone Joint*
17 *Surg Am* 1984;66:1188-97.
- 18 7. Bess S, Akbarnia BA, Thompson GH, et al. Complications of growing-rod treatment for
19 early-onset scoliosis: analysis of one hundred and forty patients. *J Bone Joint Surg Am*
20 2011;92:2533-43.
- 21 8. Cheung KM, Cheung JP, Samartzis D, et al. Magnetically controlled growing rods for
22 severe spinal curvature in young children: a prospective case series. *Lancet* 2012;379:1967-74.

- 1 9. Akbarnia BA, Cheung K, Noordeen H, et al. Next generation of growth-sparing techniques:
2 preliminary clinical results of a magnetically controlled growing rod in 14 patients with early-
3 onset scoliosis. *Spine (Phila Pa 1976)* 2013;38:665-70.
- 4 10. Samartzis D, Cheung JP, Rajasekaran S, et al. Is lumbar facet joint tropism developmental
5 or secondary to degeneration? An international, large-scale multicenter study by the AOSpine Asia
6 Pacific Research Collaboration Consortium. *Scoliosis Spinal Disord* 2016;11:9.
- 7 11. Cheung JP, Cahill P, Yaszay B, Akbarnia BA, Cheung KM. Special article: Update on the
8 magnetically controlled growing rod: tips and pitfalls. *J Orthop Surg (Hong Kong)* 2015;23:383-
9 90.
- 10 12. Cheung JPY, Yiu K, Kwan K, Cheung KMC. Mean 6-Year Follow-up of Magnetically
11 Controlled Growing Rod Patients With Early Onset Scoliosis: A Glimpse of What Happens to
12 Graduates. *Neurosurgery* 2019;84:1112-23.
- 13 13. Cheung JPY, Yiu KKL, Samartzis D, Kwan K, Tan BB, Cheung KMC. Rod Lengthening
14 With the Magnetically Controlled Growing Rod: Factors Influencing Rod Slippage and Reduced
15 Gains During Distractions. *Spine (Phila Pa 1976)* 2018;43:E399-E405.
- 16 14. Heydar AM, Sirazi S, Bezer M. Magnetic Controlled Growing Rods (MCGR) As a
17 Treatment of Early Onset Scoliosis (EOS): Early Results With Two Patients Had been Fused.
18 *Spine (Phila Pa 1976)* 2016.
- 19 15. Teoh KH, Winson DM, James SH, et al. Magnetic controlled growing rods for early-onset
20 scoliosis: a 4-year follow-up. *Spine J* 2016;16:S34-9.
- 21 16. Cheung JP, Samartzis D, Cheung KM. A novel approach to gradual correction of severe
22 spinal deformity in a pediatric patient using the magnetically-controlled growing rod. *The spine*
23 *journal : official journal of the North American Spine Society* 2014;14:e7-13.

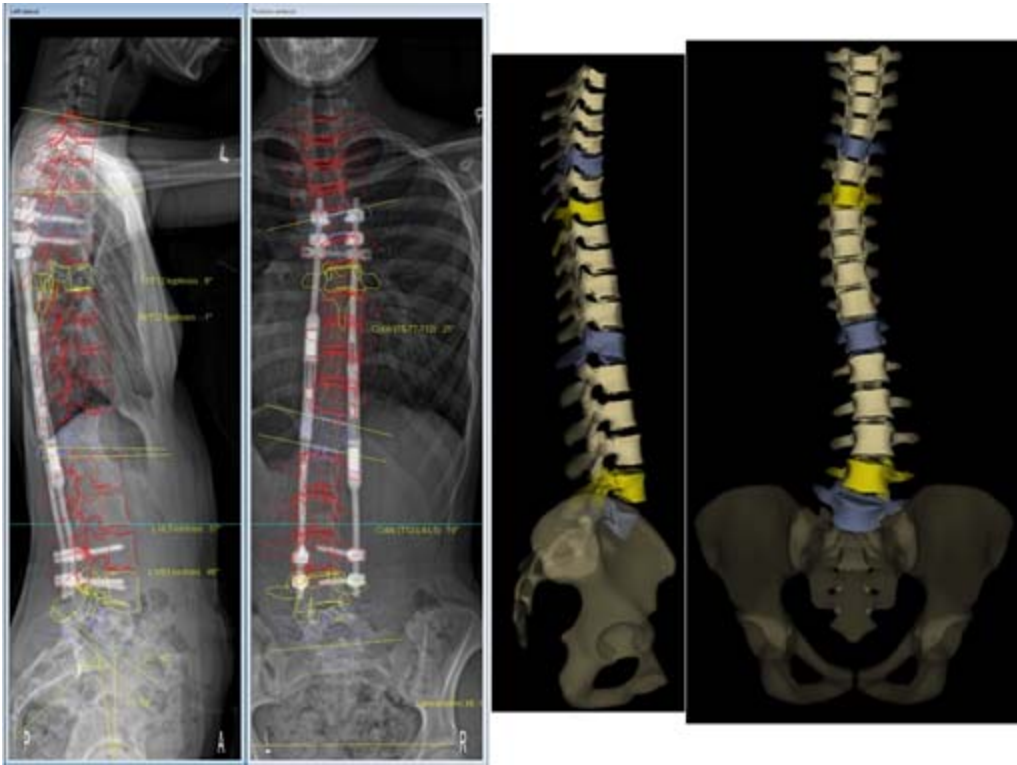
- 1 17. Kwan KYH, Cheung JPY, Yiu KKL, Cheung KMC. Ten year follow-up of Jarcho-Levin
2 syndrome with thoracic insufficiency treated by VEPTR and MCGR VEPTR hybrid. *Eur Spine J*
3 2018;27:287-91.
- 4 18. Cheung JP, Bow C, Samartzis D, Ganal-Antonio AK, Cheung KM. Clinical utility of
5 ultrasound to prospectively monitor distraction of magnetically controlled growing rods. *The spine*
6 *journal : official journal of the North American Spine Society* 2016;16:204-9.
- 7 19. Cheung JPY, Yiu KKL, Bow C, Cheung PWH, Samartzis D, Cheung KMC. Learning
8 Curve in Monitoring Magnetically Controlled Growing Rod Distractions With Ultrasound. *Spine*
9 *(Phila Pa 1976)* 2017;42:1289-94.
- 10 20. Charroin C, Abelin-Genevois K, Cunin V, et al. Direct costs associated with the
11 management of progressive early onset scoliosis: estimations based on gold standard technique or
12 with magnetically controlled growing rods. *Orthop Traumatol Surg Res* 2014;100:469-74.
- 13 21. Rushton PRP, Siddique I, Crawford R, Birch N, Gibson MJ, Hutton MJ. Magnetically
14 controlled growing rods in the treatment of early-onset scoliosis: a note of caution. *Bone Joint J*
15 2017;99-B:708-13.
- 16 22. Wong CKH, Cheung JPY, Cheung PWH, Lam CLK, Cheung KMC. Traditional growing
17 rod versus magnetically controlled growing rod for treatment of early onset scoliosis: Cost analysis
18 from implantation till skeletal maturity. *J Orthop Surg (Hong Kong)* 2017;25:2309499017705022.
- 19 23. Gunzburg R, Gunzburg J, Wagner J, Fraser RD. Radiologic interpretation of lumbar
20 vertebral rotation. *Spine (Phila Pa 1976)* 1991;16:660-4.
- 21 24. Lopez-Sosa F, Guille JT, Bowen JR. Rotation of the spine in congenital scoliosis. *J Pediatr*
22 *Orthop* 1995;15:528-34.

- 1 25. Perdriolle R, Vidal J. Thoracic idiopathic scoliosis curve evolution and prognosis. *Spine*
2 (*Phila Pa 1976*) 1985;10:785-91.
- 3 26. Krismer M, Sterzinger W, Haid C, Frischhut B, Bauer R. Axial rotation measurement of
4 scoliotic vertebrae by means of computed tomography scans. *Spine (Phila Pa 1976)* 1996;21:576-
5 81.
- 6 27. Lam GC, Hill DL, Le LH, Raso JV, Lou EH. Vertebral rotation measurement: a summary
7 and comparison of common radiographic and CT methods. *Scoliosis* 2008;3:16.
- 8 28. Gille O, Champain N, Benchikh-El-Fegoun A, Vital JM, Skalli W. Reliability of 3D
9 reconstruction of the spine of mild scoliotic patients. *Spine (Phila Pa 1976)* 2007;32:568-73.
- 10 29. Humbert L, De Guise JA, Aubert B, Godbout B, Skalli W. 3D reconstruction of the spine
11 from biplanar X-rays using parametric models based on transversal and longitudinal inferences.
12 *Med Eng Phys* 2009;31:681-7.
- 13 30. Obid P, Yiu KKL, Cheung KM, Kwan K, Ruf M, Cheung JPY. Reliability of Rod
14 Lengthening, Thoracic, and Spino-Pelvic Measurements on Biplanar Stereoradiography in
15 Patients Treated With Magnetically Controlled Growing Rods. *Spine (Phila Pa 1976)*
16 2018;43:1579-85.
- 17 31. Glaser DA, Doan J, Newton PO. Comparison of 3-dimensional spinal reconstruction
18 accuracy: biplanar radiographs with EOS versus computed tomography. *Spine (Phila Pa 1976)*
19 2012;37:1391-7.
- 20 32. Deschenes S, Charron G, Beaudoin G, et al. Diagnostic imaging of spinal deformities:
21 reducing patients radiation dose with a new slot-scanning X-ray imager. *Spine (Phila Pa 1976)*
22 2010;35:989-94.

- 1 33. Pomero V, Mitton D, Laporte S, de Guise JA, Skalli W. Fast accurate stereoradiographic
2 3D-reconstruction of the spine using a combined geometric and statistic model. *Clin Biomech*
3 (*Bristol, Avon*) 2004;19:240-7.
- 4 34. Ilharreborde B, Steffen JS, Nectoux E, et al. Angle measurement reproducibility using EOS
5 three-dimensional reconstructions in adolescent idiopathic scoliosis treated by posterior
6 instrumentation. *Spine (Phila Pa 1976)* 2011;36:E1306-13.
- 7 35. Glattes RC, Bridwell KH, Lenke LG, Kim YJ, Rinella A, Edwards C, 2nd. Proximal
8 junctional kyphosis in adult spinal deformity following long instrumented posterior spinal fusion:
9 incidence, outcomes, and risk factor analysis. *Spine (Phila Pa 1976)* 2005;30:1643-9.
- 10 36. Cohen J, Cohen P, West SG, Aiken LS. Applied multiple regression/correlation analysis
11 for the behavioral sciences. . Third ed. New Jersey: Lawrence Erlbaum Associates.; 2003.
- 12 37. Acaroglu E, Yazici M, Alanay A, Surat A. Three-dimensional evolution of scoliotic curve
13 during instrumentation without fusion in young children. *J Pediatr Orthop* 2002;22:492-6.
- 14 38. Kamaci S, Demirkiran G, Ismayilov V, Olgun ZD, Yazici M. The effect of dual growing
15 rod instrumentation on the apical vertebral rotation in early-onset idiopathic scoliosis. *J Pediatr*
16 *Orthop* 2014;34:607-12.
- 17 39. Sangole AP, Aubin CE, Labelle H, et al. Three-dimensional classification of thoracic
18 scoliotic curves. *Spine (Phila Pa 1976)* 2009;34:91-9.
- 19 40. Luk KD, Cheung WY, Wong Y, Cheung KM, Wong YW, Samartzis D. The predictive
20 value of the fulcrum bending radiograph in spontaneous apical vertebral derotation in adolescent
21 idiopathic scoliosis. *Spine (Phila Pa 1976)* 2012;37:E922-6.

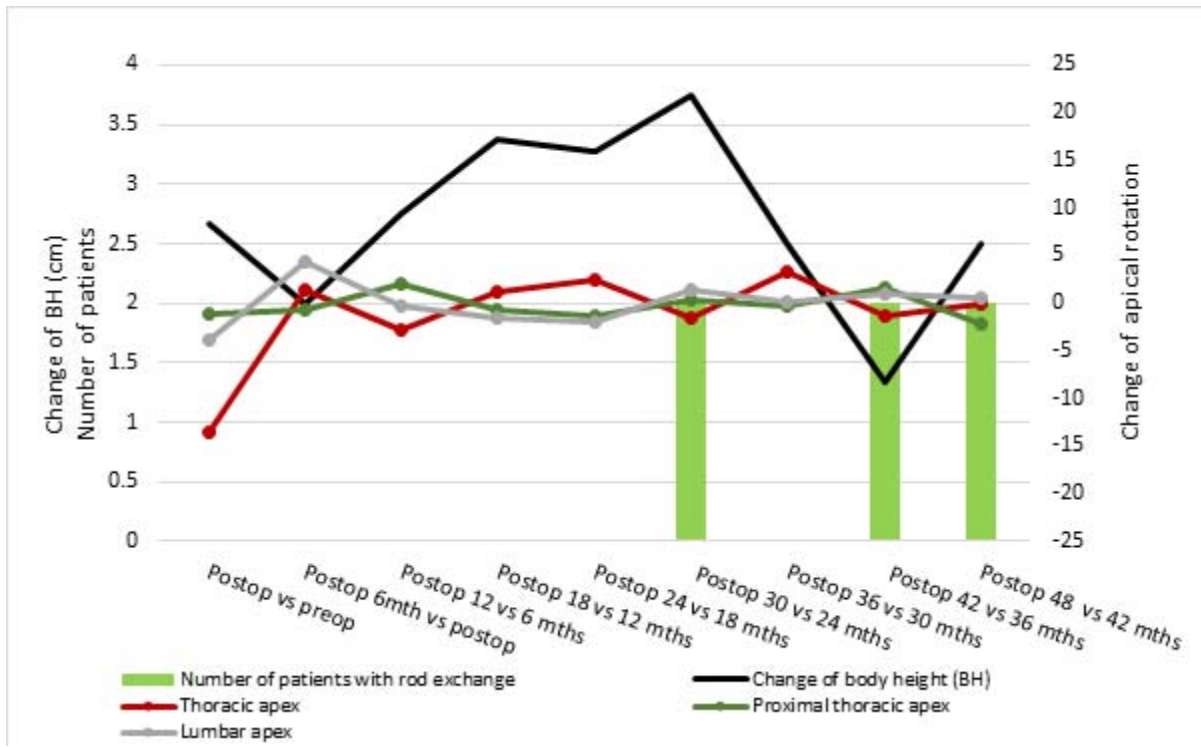
- 1 41. Luk KD, Vidyadhara S, Lu DS, Wong YW, Cheung WY, Cheung KM. Coupling between
2 sagittal and frontal plane deformity correction in idiopathic thoracic scoliosis and its relationship
3 with postoperative sagittal alignment. *Spine (Phila Pa 1976)* 2010;35:1158-64.
- 4 42. Yao G, Cheung JPY, Shigematsu H, et al. Characterization and Predictive Value of
5 Segmental Curve Flexibility in Adolescent Idiopathic Scoliosis Patients. *Spine (Phila Pa 1976)*
6 2017;42:1622-8.
- 7 43. Kwan KYH, Alanay A, Yazici M, et al. Unplanned Reoperations in Magnetically
8 Controlled Growing Rod Surgery for Early Onset Scoliosis with a Minimum of Two-Year Follow-
9 Up. *Spine (Phila Pa 1976)* 2017.
- 10 44. Lebon J, Batailler C, Wargny M, et al. Magnetically controlled growing rod in early onset
11 scoliosis: a 30-case multicenter study. *Eur Spine J* 2016.

1 **Figure Legends**



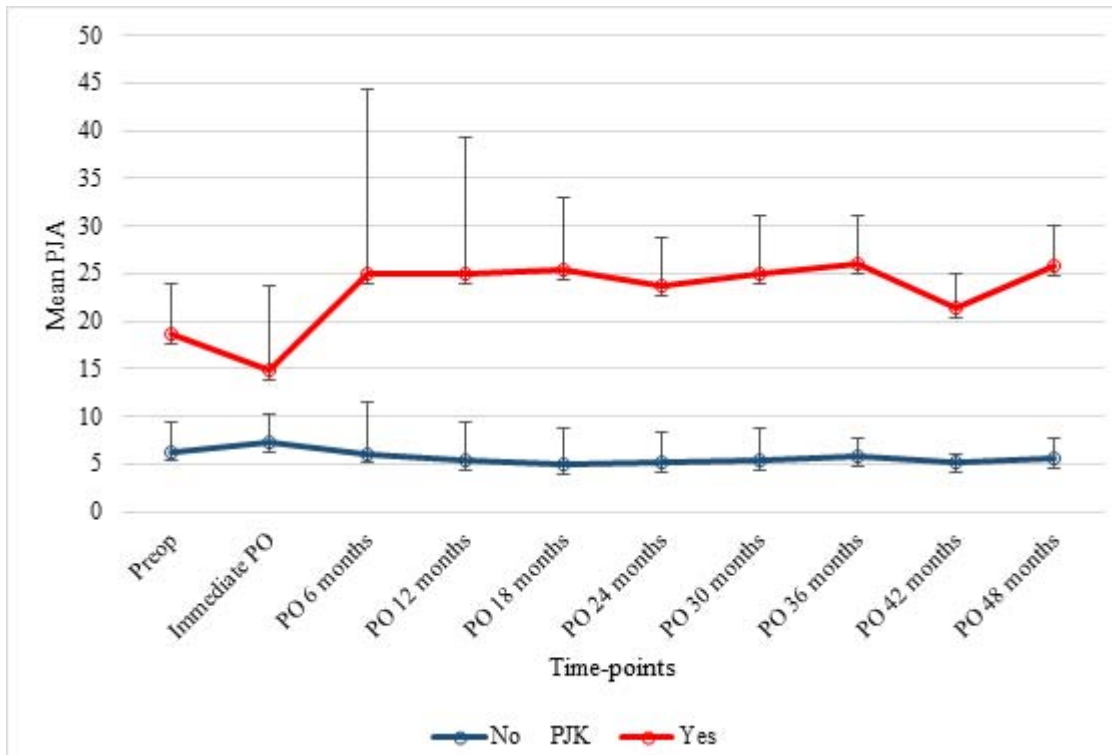
2

3 **Figure 1:** 3D reconstruction output created from SterEOS®.



1

2 **Figure 2:** Graph of the changes in rotational profile at the proximal thoracic, thoracic and lumbar
 3 apices with initial implantation and at every 6 months follow-up. The main change occurs at
 4 initiation implantation and no significant deviations are observed thereafter despite growth or with
 5 rod exchange.



1

2 **Figure 3:** Mean changes with standard deviation bars for proximal junctional angle (PJA) in
 3 degrees at preop, immediate postop (PO), PO 6 months, PO 12 months, PO 18 months, PO 24
 4 months, PO 30 months, PO 36 months, PO 42 months and PO 48 months between patients with
 5 and without proximal junctional kyphosis (PJK).

1 **Table Legends**

2 **Table 1:** Patient profiles.

3 **Table 2:** Baseline radiological parameters.

4 **Table 3:** Changes of growth and clinical parameters between time-points.

5 **Table 4:** Correlation tests of changes of Cobb angles, changes of sagittal parameters and changes
6 rotational profiles at all time-points.

7 **Table 5:** Proximal junctional angle (mean values \pm SD) at specific time-points.

8 **Table 6:** Changes of Proximal junctional angle (mean values \pm SD) at specific time-points.

Table 1: Patient profiles

Subject Number	Gender	Diagnosis	Age at MCGR Implantation (years)	Foundations	Complications	Number of rod exchanges (years after first surgery)	Unplanned Reoperation
#01	F	Juvenile idiopathic scoliosis	8.5	T4/5 upgoing pedicle hooks, L2/3 pedicle screws	Nil	1 (3yrs)	
#02	F	Juvenile idiopathic scoliosis	12.7	T3/4 claw construct, L2/3 pedicle screws	Nil	0	
#03	F	Infantile idiopathic scoliosis with Marfanoid features	4.1	T4/5, L3/4 pedicle screws	Nil	1 (3yrs)	
#04	F	Arthrogyposis	9.4	T3/4 upgoing pedicle hooks, L2/3 pedicle screws	Nil	0	
#05	F	Juvenile idiopathic scoliosis with Marfanoid features	7.4	T4/5, L3/4 pedicle screws	Proximal foundation nonunion, anchor loosening, bone formation at expandable portion of rod, PJK	1 (2yrs)	2 (proximal foundation nonunion and anchor loosening)
#06	F	Sotos syndrome	4.3	T5/6 claw construct, L3/4 pedicle screws	Bone formation at expandable portion of rod, metallosis, PJK	1 (4yrs)	
#07	F	Juvenile idiopathic scoliosis	11.4	T5/6, L3/4 pedicle screws	Broken rod, metallosis	1 (2yrs)	1 (broken rod, metallosis)
#08	M	Neurofibromatosis scoliosis	4.8	T3/4, L3/4 pedicle screws	Infection, PJK	2 (2yrs, 4yrs)	1 (infection)
#09	F	Neuromuscular scoliosis	10.4	T1/2, L1/2 pedicle screws	Nil	0	
#10	M	Juvenile idiopathic scoliosis	9.0	T5/6 upgoing pedicle hooks, L2/3 pedicle screws	Nil	0	

Table 2: Baseline radiological parameters

Parameters	Mean \pm SD
Imaging parameters	
Preoperative curve magnitude - Cobb angle (degrees)	
Thoracic	68.7 \pm 18.3
Proximal thoracic	15.9 \pm 20.6
Lumbar	39.7 \pm 4.0
Proximal junctional angle	8.1 \pm 4.6
Preoperative sagittal profile	
T1-T12 kyphosis	31.3 \pm 13.3
T4-T12 kyphosis	29.0 \pm 15.4
L1-S1 lordosis	58.0 \pm 6.2
L1-L5 lordosis	41.5 \pm 7.0
Preoperative pelvic profile	
Pelvic tilt - Sagittal	4.7 \pm 14.8
- Lateral	7.0 \pm 4.4
Pelvic incidence	48.6 \pm 13.2
Sacral slope	43.9 \pm 5.8
Pelvis rotation	-1.0 \pm 4.4
Preoperative rotational profile – apical vertebral rotation	
Thoracic apex	-13.7 \pm 10.5
Proximal thoracic apex	0.9 \pm 1.4
Lumbar apex	5.2 \pm 12.1

Table 3: Changes of growth and clinical parameters between time-points

Parameters (Mean ± SD)	Immediate postop vs preop	Postop 6 months vs immediate postop	12 vs 6 months	18 vs 12 months	24 vs 18 months	30 vs 24 months	36 vs 30 months	42 vs 36 months	48 vs 42 months	p-value
Changes of growth parameters mean ± SD)										
Body Height (cm)	2.7 ± 1.5	2.0 ± 1.4	2.8 ± 0.5	3.4 ± 2.4	3.3 ± 1.2	3.8 ± 1.0	2.5 ± 0.6	1.3 ± 1.2	2.5 ± 2.1	0.371
Body Weight (kg)	0.5 ± 0.7	2.0 ± 1.7	-0.2 ± 1.0	1.5 ± 0.4	1.4 ± 2.2	1.4 ± 1.3	1.5 ± 1.9	1.6 ± 1.9	1.3 ± 1.5	0.765
Arm span (cm)	1.0 ± 0.0	4.0 ± 2.2	2.9 ± 0.9	2.8 ± 1.8	3.1 ± 1.1	3.3 ± 1.7	3.1 ± 1.5	1.0 ± 0.9	3.0 ± 0.0	0.004*
BMI	-0.4 ± 0.6	0.7 ± 0.8	-0.8 ± 0.6	0.1 ± 0.8	0.0 ± 0.9	0.1 ± 0.9	0.3 ± 0.9	0.4 ± 0.7	0.2 ± 0.4	0.785
Changes of Cobb angles (degree, mean ± SD)										
Thoracic	-45.7 ± 24.4	3.5 ± 5.4	0.1 ± 1.3	1.3 ± 2.3	0.4 ± 4.0	-2.2 ± 1.2	-1.6 ± 3.5	0.6 ± 1.2	0.4 ± 1.6	<0.001*
Proximal thoracic	-12.7 ± 17.9	-2.0 ± 3.0	-0.4 ± 3.8	1.0 ± 3.8	0.2 ± 3.0	4.4 ± 3.1	0.5 ± 5.5	2.3 ± 4.4	3.6 ± 0.4	0.158
Lumbar	-26.7 ± 7.1	2.3 ± 7.8	1.5 ± 3.5	-1.7 ± 2.7	-1.4 ± 0.4	-1.8 ± 2.4	1.8 ± 3.3	-0.5 ± 0.7	-2.5 ± 3.5	<0.001*
Proximal junctional angle	-0.8 ± 3.6	2.6 ± 8.2	-0.3 ± 4.0	0.0 ± 4.0	-0.6 ± 3.6	0.4 ± 3.1	0.5 ± 2.7	-1.8 ± 2.4	2.0 ± 2.8	0.532
Sagittal Profile changes										
T1-T12 kyphosis	-3.3 ± 1.4	8.2 ± 12.8	4.6 ± 7.8	2.8 ± 6.9	-1.4 ± 5.0	-3.2 ± 9.8	-3.2 ± 6.4	4.7 ± 1.3	-2.2 ± 5.7	0.393
T4-T12 kyphosis	-6.2 ± 10.8	5.3 ± 8.0	4.5 ± 3.7	-5.0 ± 2.0	1.6 ± 8.0	1.1 ± 2.5	0.9 ± 2.8	0.7 ± 4.5	1.5 ± 1.3	0.282
L1-S1 lordosis	-10.4 ± 14.1	5.7 ± 10.3	6.6 ± 9.8	4.5 ± 4.8	-2.6 ± 4.6	6.9 ± 8.0	-3.9 ± 9.0	2.0 ± 3.3	1.0 ± 3.8	0.256
L1-L5 lordosis	-7.3 ± 9.3	7.3 ± 4.2	2.8 ± 4.8	2.5 ± 4.0	-0.2 ± 2.3	3.8 ± 4.0	-1.1 ± 8.0	2.2 ± 1.6	0.6 ± 1.9	0.167
Rotational profile changes										
Thoracic apex	-13.6 ± 11.4	1.5 ± 5.2	-2.7 ± 5.1	1.2 ± 4.5	2.5 ± 5.6	-1.6 ± 3.1	3.4 ± 3.5	-1.3 ± 1.5	-0.1 ± 1.1	0.042*
Proximal thoracic apex	-1.1 ± 1.5	-0.6 ± 7.3	2.1 ± 4.6	-0.6 ± 5.2	-1.4 ± 3.1	0.4 ± 9.5	-0.2 ± 7.5	1.6 ± 2.3	-2.1 ± 3.0	0.991
Lumbar apex	-3.8 ± 2.0	4.3 ± 6.8	-0.2 ± 5.4	-1.6 ± 3.6	-1.9 ± 5.1	1.4 ± 3.7	0.2 ± 2.6	1.0 ± 2.7	0.5 ± 0.7	0.574
Pelvic parameters (mean ± SD, degrees)										
Sagittal pelvic tilt	7.4 ± 10.7	-4.0 ± 7.8	-2.7 ± 10.3	-2.4 ± 7.9	-1.7 ± 7.1	-0.6 ± 8.4	0.9 ± 8.8	0.3 ± 3.4	-0.1 ± 6.8	0.903
Lateral pelvic tilt	2.0 ± 4.2	0.8 ± 1.7	-0.3 ± 2.6	-0.7 ± 1.2	0.3 ± 0.5	-0.5 ± 2.1	0.0 ± 3.5	-1.7 ± 1.2	2.5 ± 2.1	0.664
Pelvis rotation	6.3 ± 0.6	-2.1 ± 9.0	0.5 ± 5.9	-1.9 ± 1.4	2.4 ± 1.7	0.8 ± 1.5	0.2 ± 4.0	-0.9 ± 2.2	3.0 ± 0.3	0.602

BMI: body mass index

Table 4: Changes between preoperative, immediate postoperative and final follow-up measurements

Parameters	Mean pre-operative (±SD)	Mean immediate postoperative (±SD)	Mean final follow-up (±SD)	Preoperative vs Final p-value	Immediate postop vs Final p-value
Cobb Angle					
Thoracic	68.7±18.3	23.8±10.7	19.2±9.6	0.005*	0.543
Proximal thoracic	15.9±20.6	15.6±13.8	18.5±1.2	0.851	0.692
Lumbar	39.7±4.0	9.1±7.6	9.0±8.2	0.002*	0.979
Proximal junctional angle	8.1±4.6	7.3±4.8	12.9±8.7	0.359	0.322
Sagittal Profile					
T1-T12 kyphosis	31.3±13.3	33.5±20.4	44.1±16.7	0.327	0.451
T4-T12 kyphosis	29.0±15.4	29.9±17.2	33.3±20.1	0.772	0.806
L1-S1 lordosis	58.0±6.2	42.9±18.8	44.1±6.4	0.034*	0.912
L1-L5 lordosis	41.5±7.0	30.3±13.5	31.6±7.3	0.130	0.876
Rotational Profile					
Thoracic apex	-13.7±10.5	-11.2±16.6	1.9±15.5	0.197	0.292
Proximal thoracic apex	0.9±1.4	1.5±1.5	2.0±5.4	0.748	0.864
Lumbar apex	5.2±12.1	-1.6±5.3	8.6±7.7	0.664	0.072
Pelvic parameters					
Sagittal pelvic tilt	4.7±14.8	8.3±13.7	6.8±8.2	0.816	0.862
Lateral pelvic tilt	7.0±4.4	5.3±6.7	3.8±1.3	0.325	0.673
Pelvis rotation	-1.0±4.4	0.7±6.0	0.3±4.9	0.742	0.916

Commented [PC1]: Paired samples t-test

Table 4: Correlation tests of changes of Cobb angles, changes of sagittal parameters and changes rotational profiles at all time-points

Changes between time-points	r_s	p-value	r_s	p-value	r_s	p-value	r_s	p-value
	Coronal parameters							
	Thoracic Cobb angle		Proximal Thoracic Cobb angle		Lumbar Cobb angle		Proximal junctional angle	
Vertebral rotation at thoracic apex	0.191	0.320	0.278	0.145	0.228	0.235	-0.094	0.626
Sagittal Parameters								
T1-T12 kyphosis	0.496	0.006**	-0.210	0.274	0.116	0.550	-0.198	0.304
T4-T12 kyphosis	0.174	0.368	-0.359	0.056	0.286	0.133	0.184	0.339
L1-S1 lordosis	0.406	0.029*	0.042	0.831	-0.080	0.681	0.138	0.475
L1-L5 lordosis	0.330	0.081	-0.074	0.701	-0.098	0.613	-0.370	0.048*

Table 5: Proximal junctional angle (mean values \pm SD) at specific time-points

PJA	Preoperative	Immediate PO	PO 6 months	PO 12 months	PO 18 months	PO 24 months	PO 30 months	PO 36 months	PO 42 months	PO 48 months
>10° (n=3)	12.3 \pm 5.3	7.7 \pm 8.8	18.8 \pm 19.4	19.5 \pm 14.4	20.3 \pm 7.6	18.5 \pm 5.0	19.6 \pm 6.1	20.2 \pm 5.1	16.1 \pm 3.6	20.3 \pm 4.2
<10° (n=7)	6.3 \pm 3.0	7.2 \pm 3.1	6.1 \pm 5.3	5.4 \pm 3.9	5.0 \pm 3.8	5.2 \pm 3.1	5.3 \pm 3.5	5.8 \pm 1.8	5.2 \pm 0.8	5.5 \pm 2.3
p-value	0.067	0.667	0.517	0.183	0.033*	0.024*	0.024*	0.024*	0.024*	0.100

PJA: proximal junctional angle; PO: postoperative

Table 6: Changes of Proximal junctional angle (mean values \pm SD) at specific time-points

PJA	Preop vs Immediate PO	PO 6 months vs Immediate PO	PO 12 vs 6 months	PO 18 vs 12 months	PO 24 vs 18 months	PO 30 vs 24 months	PO 36 v 30 months	PO 42 vs 36 months	PO 48 vs 42 months
>10° (n=3)	-4.6 \pm 3.7	11.1 \pm 10.8	0.7 \pm 6.4	0.8 \pm 6.8	-1.8 \pm 6.5	1.1 \pm 6.0	0.6 \pm 3.3	-4.1 \pm 1.5	4.2 \pm 0.6
<10° (n=7)	0.9 \pm 2.1	-1.1 \pm 3.3	-0.7 \pm 3.1	-0.4 \pm 2.8	0.0 \pm 1.8	0.1 \pm 0.9	0.5 \pm 2.7	-0.6 \pm 1.8	-0.2 \pm 2.4
p-value	0.033*	0.033*	0.517	0.833	0.714	1.000	1.000	0.048*	0.100

PJA: proximal junctional angle; PO: postoperative